Supplementary data for:

Glacial-Interglacial changes and Holocene variations in Arabian Sea denitrification

Birgit Gaye[1], Anna Böll[1], Joachim Segschneider[2], Nicole Burdanowitz[1], Kay-Christian Emeis[1,3], Venkitasubramani Ramaswamy[4], Niko Lahajnar[1], Andreas Lückge[5] and Tim Rixen[1,6]

[1]Institute for Geology, Universität Hamburg, Bundesstraße 55, 20146 Hamburg, Germany
[2]Institute for Geosciences, Universität Kiel, Ludewig-Meyn-Straße 10, 24118 Kiel, Germany
[3]Institute of Coastal Research, Helmholtz Center Geesthacht, Max-Planck-Straße 1, 21502 Geesthacht, Germany
[4]National Institute of Oceanography, Dona Paula, Goa, 403004, India
[5]Bundesanstalt für Geowissenschaften und Rohstoffe, Stilleweg 2, 30655 Hannover, Germany
[6]Leibniz-Zentrum für Marine Tropenforschung (ZMT) GmbH, Fahrenheitstraße 6, 28359 Bremen, Germany

Table S1 provides $\delta^{15}N$ data and their regional averages. References for original literature data are in Table 1.

Table S2 provides original SST data and their regional averages. References for original literature data are in Table 1.

Table S3 provides data of radiocarbon AMS datings for Arabian Sea cores SL163 and MC681 and **Figure S3** shows the age model for combined gravity core SL163 and multicore MC681 taken at the same location.

Table S4 provides data of radiocarbon AMS datings for Arabian Sea core MC680 and **Figure S4** shows the age model for MC680.

Figure S5: KCM-PISCES simulated (average over the last 20 years of the experiment representing 0 ka , solid) and present day World Ocean Atlas (dashed, WOA13, Garcia et al. 2014) observation based oxygen concentration versus depth as average over the Arabian Sea

(55°E-75°E, 8.5°N-26°N). The simulated oxygen concentration at the surface is too high due to a cold bias in KCM compared to present day observed temperatures, resulting in generally too high oxygen concentrations, but the near surface gradient is well matched. In the deep ocean, more oxygen than observed is brought into the Arabian Sea by the deep circulation.

Figure S6: Horizontal distribution of the observation based (WOA2013, Garcia et al.,2014) oxygen concentration at the depth of the simulated minimum oxygen concentration (217m) from WOA data interpolated to model levels, based on the 1°x1° annual mean data.

Figure S7: same as Fig. 4, but for the KCM-PISCES control simulation interpolated to a 1°x1° grid. While oxygen concentrations are generally too high for reasons pointed out in the caption of Fig. 3, the lowest concentrations are in the eastern Arabian Sea as observed. Despite the deficiencies the simulation of the Arabian Sea is in the range of large scale global models and we claim that it can be used to estimate the temporal evolution of the Arabian Sea over the Holocene at least qualitatively as done here.

Figure S8: SST in cores of high resolution form the northern Arabian Sea (SP90-136KL; (Schulte and Muller, 2001), Oman upwelling (MD00-2354; (Böll et al., 2015), the Somali upwelling (TY93-929; (Tierney et al., 2016), and the eastern Arabian Sea (SK237-GC04; (Saraswat et al., 2013). Warm IS (IS1, IS2) and cold stadials (YD, H1) are marked by letters and grey bars.

Figure S9: $\delta^{15}N$ in cores of high resolution from the northern Arabian Sea (SO90-111KL; (Suthhof et al., 2001), Oman upwelling (RC27-23; (Altabet et al., 2002), and Somali upwelling (NIOP-905P; (Ivanochko et al., 2005). Warm IS (IS1, IS2) and cold stadials (YD, H1) are marked by letters and grey bars.

Table S3

Results of radiocarbon AMS datings. Beta refers to Beta Analytics, Miami, FL/USA, KIA to the Leibniz Laboratory, Kiel/Germany and ETH to the ETH Laboratory of Ion Beam Physics, Zurich/Switzerland

Core	Depth (cmbsf)	Lab Code	Material	Conventional 14C age (yr BP)	Reservoir corrected calibrated age (cal BP)
MC681	1 ± 1	Beta342813	mixed planktics	650 ± 30	30 ± 30
MC681	1 ± 1	Beta342812	bulk organic fraction	630 ± 30	10 ± 30
MC681	11.5 ± 0.5	Beta342814	bulk organic fraction	1300 ± 30	584 ± 84
MC681	33.5 ± 0.5	Beta342815	bulk organic fraction	1960 ± 30	1202 ± 125
163SL	22.5 ± 0	ETH	N.dutertrei	1996 ± 67	1234.5 ± 182.5
163SL	31.5 ± 0.5	Beta346602	bulk organic fraction	1980 ± 30	1226 ± 126
163SL	52.5 ± 0.5	Beta346603	bulk organic fraction	2100 ± 30	1372.5 ± 123.5
163SL	58.5 ± 0.5	Beta346604	bulk organic fraction	5740 ± 30	5798 ± 139
163SL	77.75 ± 1.25	KIA47119	N.dutertrei	5760 ± 30	5832.5 ± 142.5
163SL	141.25 ± 1.25	Beta319751	N.dutertrei	5990 ± 30	6097 ± 149
163SL	193.75 ± 1.25	Beta319752	N.dutertrei	6350 ± 40	6474 ± 156
163SL	252.75 ± 2.75	KIA47120	N.dutertrei	6715 ± 35	6909.5 ± 177.5
163SL	278.75 ± 1.25	Beta319753	N.dutertrei	6670 ± 40	6839 ± 170
163SL	295 ± 0	Beta319754	N.dutertrei	7030 ± 40	7274 ± 129
163SL	326.25 ± 1.25	Beta319755	N.dutertrei	6990 ± 40	7223.5 ± 155.5
163SL	353.75 ± 1.25	KIA47121	N.dutertrei	7420 ± 40	7598 ± 128
163SL	392.5 ± 0	KIA47122	N.dutertrei	8090 ± 40	8257.5 ± 133.5
163SL	395 ± 0	Beta319756	N.dutertrei	8090 ± 40	8257.5 ± 133.5
163SL	417.5 ± 0	Beta342816	N.dutertrei	8500 ± 40	8740 ± 200

Figure S3:
Age model for SL163/MC681

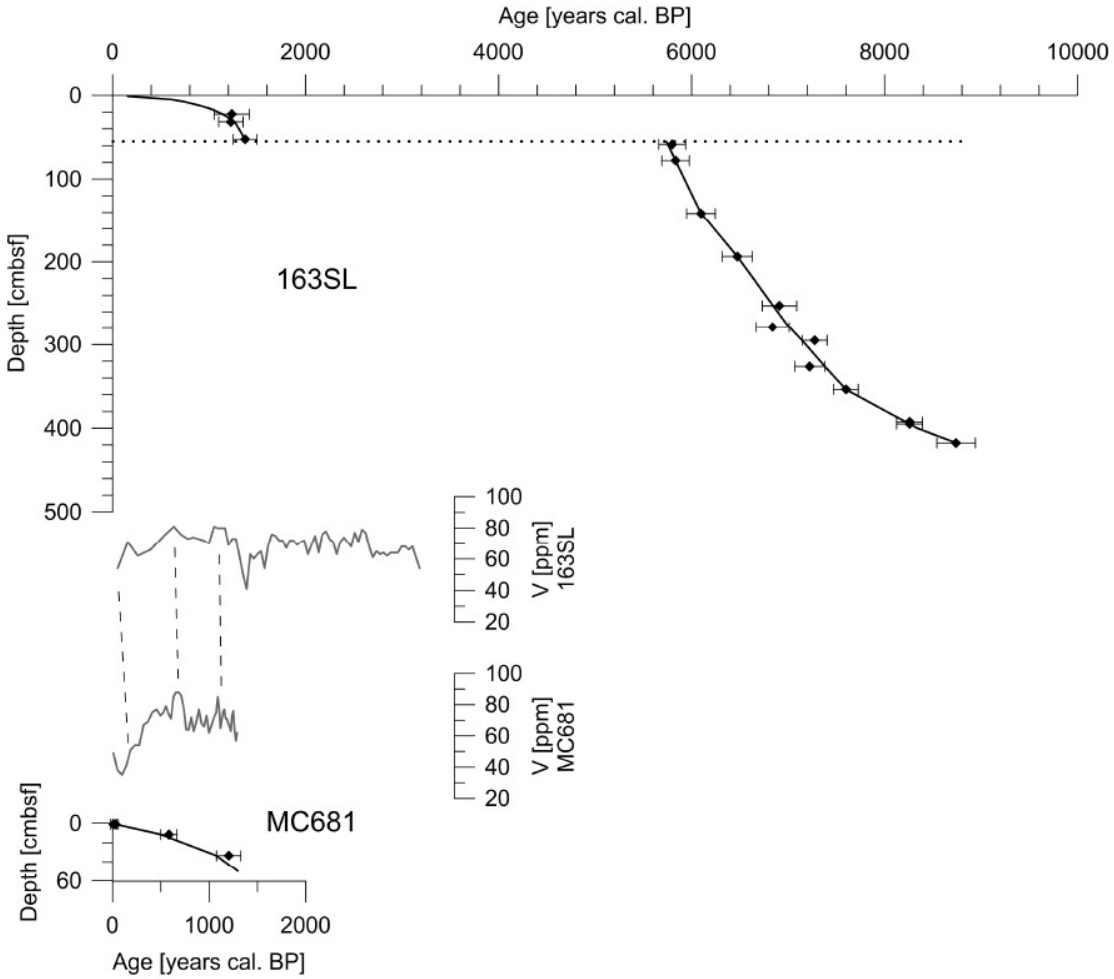

Table S4

Results of radiocarbon AMS datings. Beta refers to Beta Analytics, Miami, FL/USA

Core	Depth (cmbsf)	Lab Code	Material	Conventional ^{14}C age (yr BP)	Reservoir corrected calibrated age (cal BP)
MC680	1 ± 1	Beta340286	mixed planktics	80 ± 30	post 1950
MC680	12 ± 2	Beta357279	N.dutertrei	600 ± 30	15 ± 38
MC680	20.5 ± 1.5	Beta357280	mixed planktics	810 ± 30	239 ± 179
MC680	40 ± 1	Beta357281	mixed planktics	5600 ± 40	5758 ± 156

Figure S4:
Age model for MC680

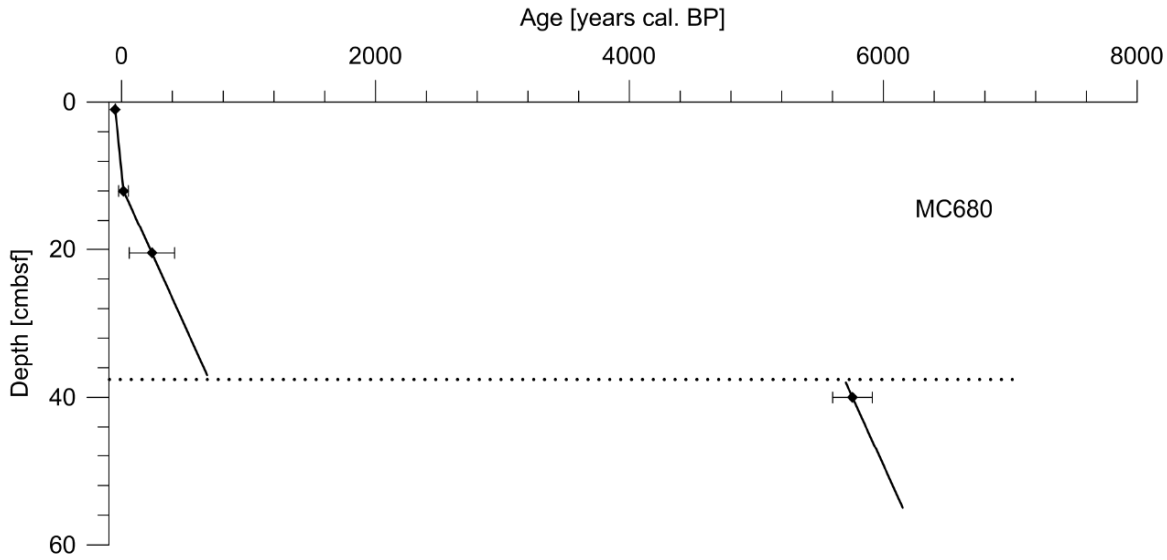

Figure S5:

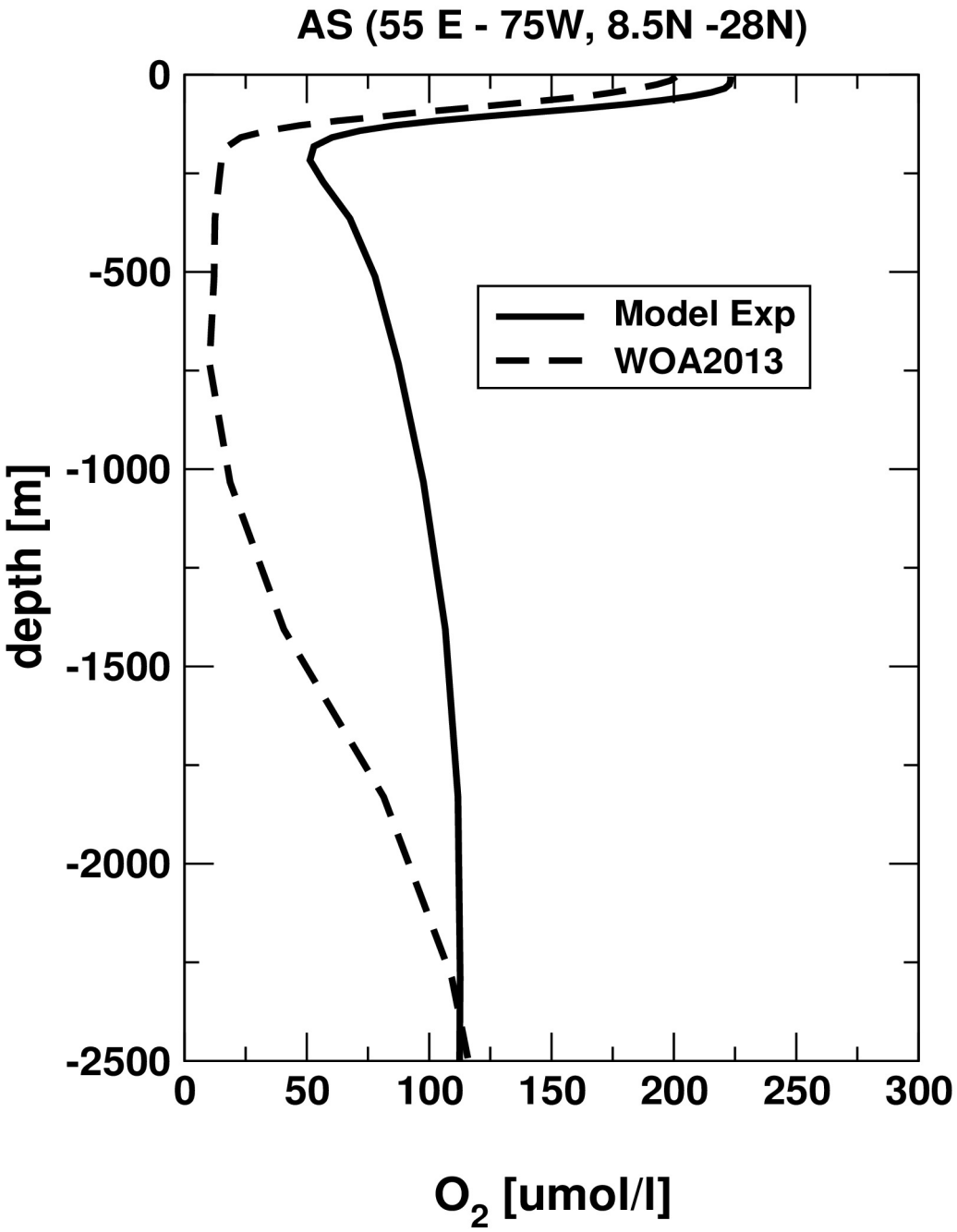
AS (55 E - 75W, 8.5N -28N)
0
-500
-1000
-1500
-2000
-2500
depth [m]
0
50
100
150
200
250
300
O2 [umol/l]
Model Exp
WOA2013

Figure S6:

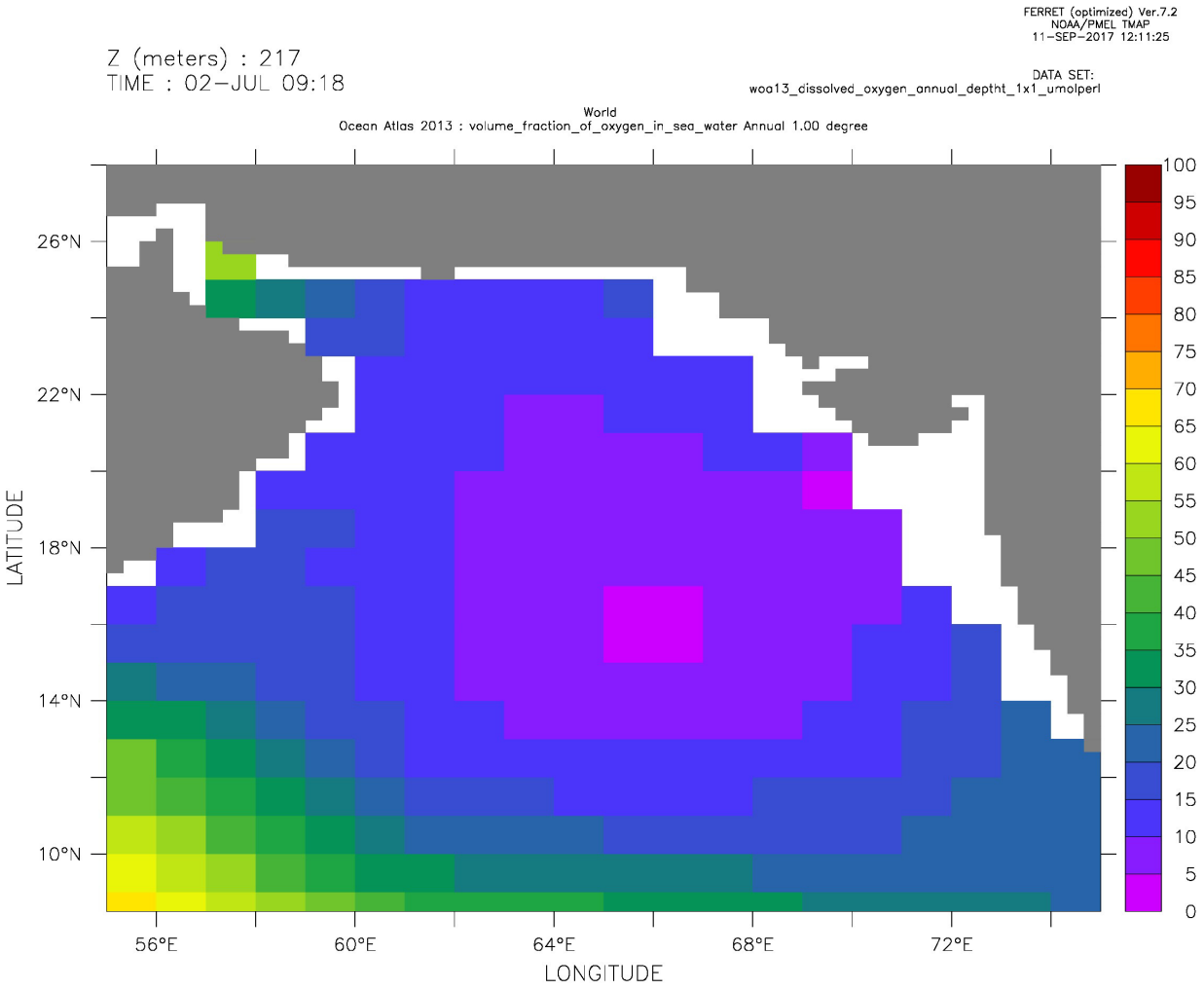

Objectively analyzed mean fields for volume_fraction_of_oxygen_in_sea_water at standard depth levels. (umol/l)

Figure S7:

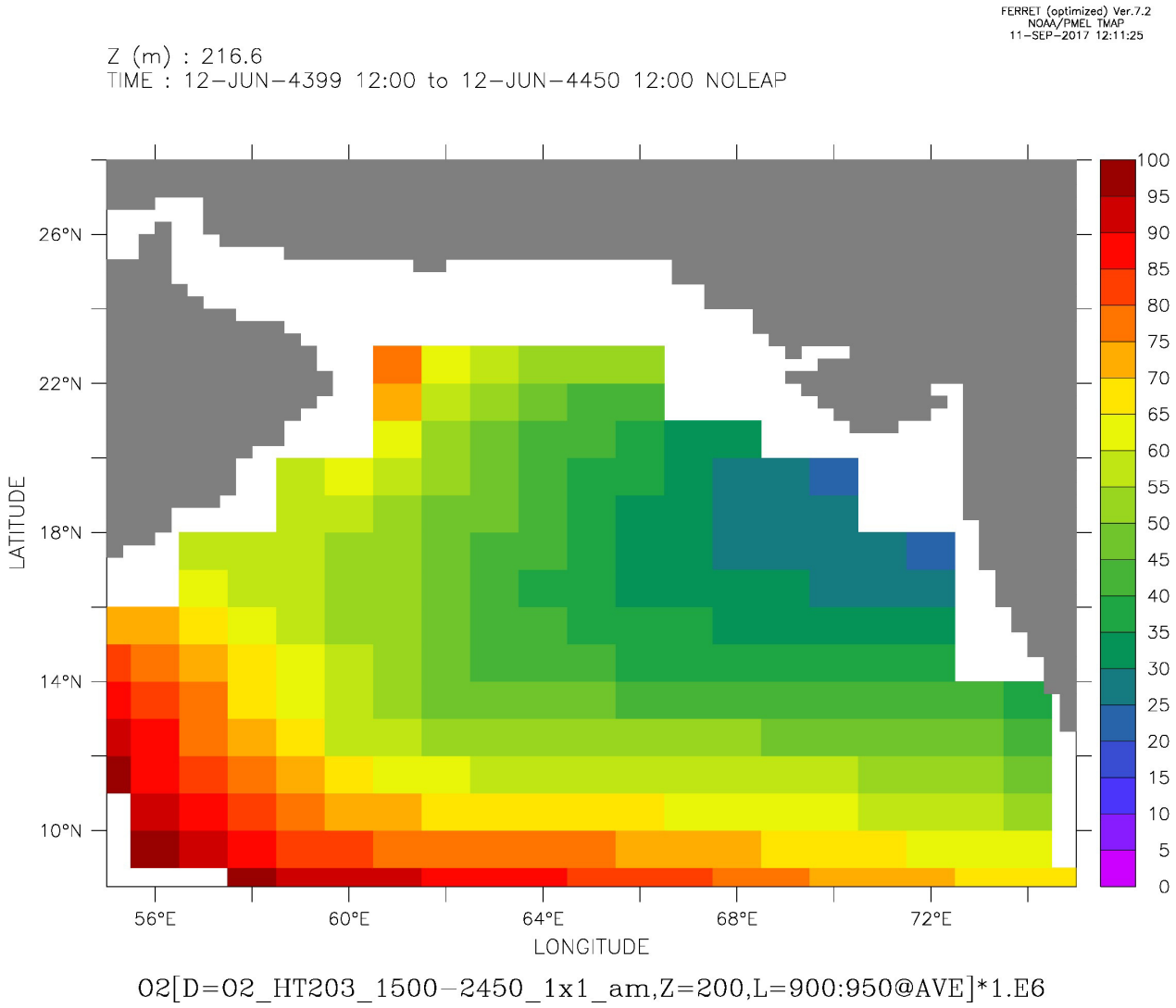
FERRET (optimized) Ver.7.2
NOAA/PMEL TMAP
11-SEP-2017 12:11:25
Z (m) : 216.6
TIME : 12-JUN-4399 12:00 to 12-JUN-4450 12:00 NOLEAP
26°N
22°N
18°N
14°N
10°N
LATITUDE
56°E
60°E
64°E
68°E
72°E
LONGITUDE
100
95
90
85
80
75
70
65
60
55
50
45
40
35
30
25
20
15
10
5
0
02[D=02_HT203_1500-2450_1x1_am,Z=200,L=900:950@AVE]*1.E6

Figure S8:

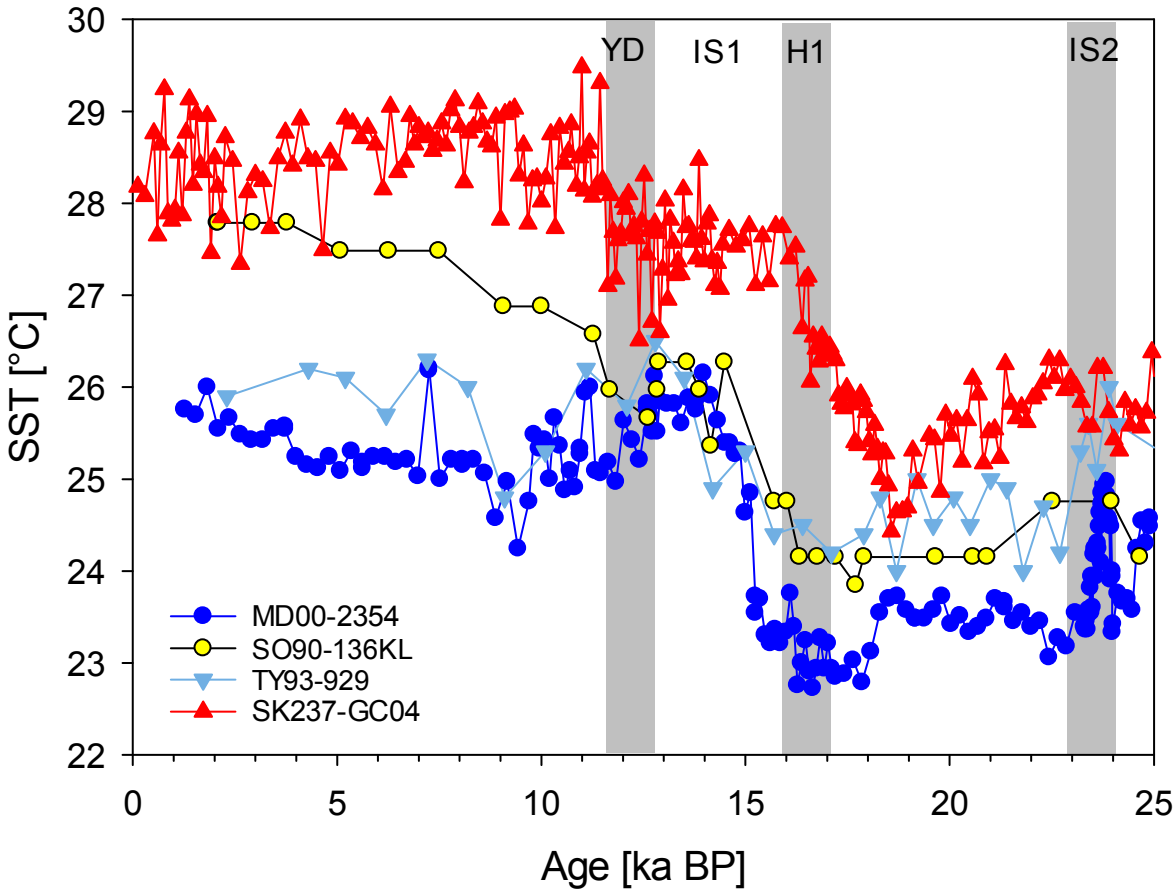
YD
IS1
H1
IS2
SST [°C]
Age [ka BP]
MD00-2354
SO90-136KL
TY93-929
SK237-GC04

Figure S9:

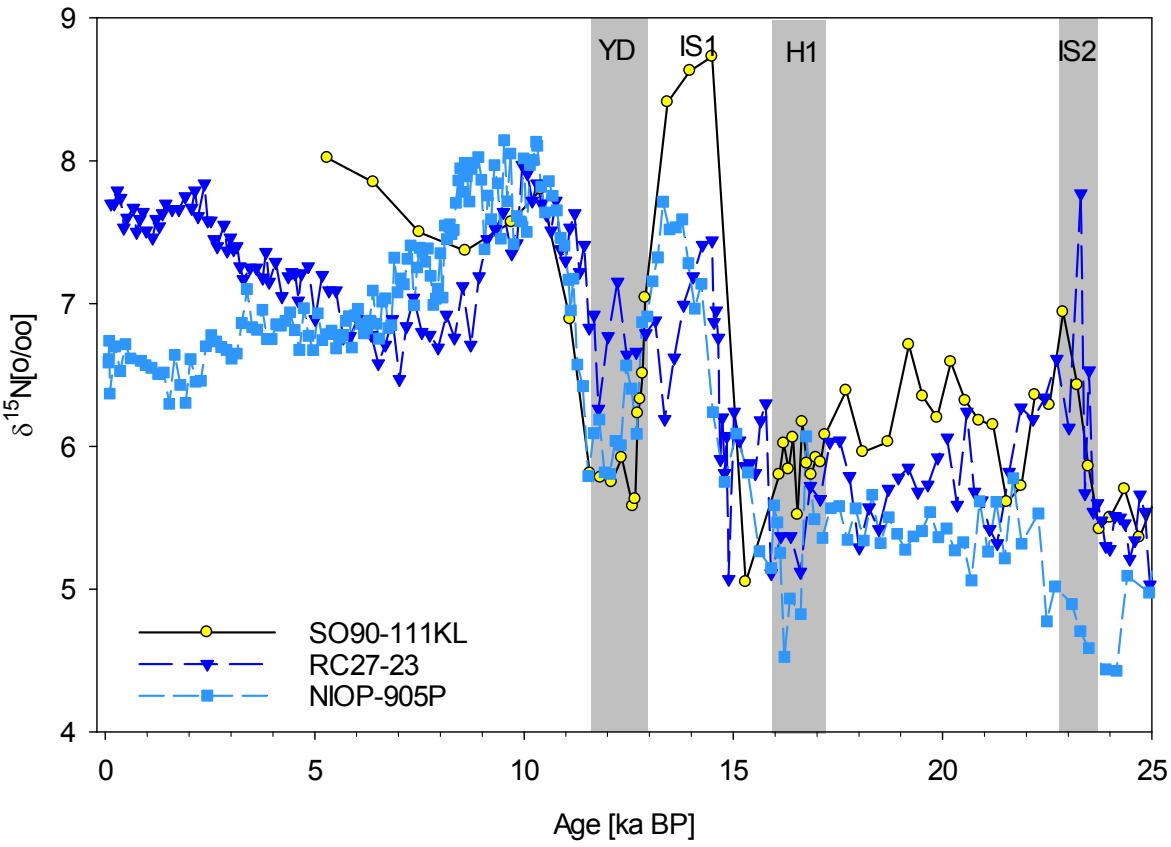
YD
IS1
H1
IS2
SO90-111KL
RC27-23
NIOP-905P
δ15N[o/oo]
Age [ka BP]
9
8
7
6
5
4
0
5
10
15
20
25

References

Altabet, M. A., Higginson, M. J., and Murray, D. W.: The effect of millennial-scale changes in Arabian Sea denitrification on atmospheric CO_2, Nature, 415, 159-162, 2002.

Böll, A., Schulz, H., Munz, P., Rixen, T., Gaye, B., and Emeis, K.-C.: Contrasting sea surface temperature of summer and winter monsoon variability in the northern Arabian Sea over the last 25ka, Palaeogeography, Palaeoclimatology, Palaeoecology, 426, 10-21, 2015.

Garcia, H.E., Locarnini, R.A., Boyer, T.P., Antonov, J.I., Baranova, M.M., Reagan, J.R., and Johnson, D.R.: World Ocean Atlas 2013, Volume 3: Dissolved Oxygen, Apparent Oxygen Utilization, and Oxygen Saturation. S. Levitus, Ed., A. Mishonov Technical Ed.; NOAA Atlas NESDIS 76, 25pp, 2014.

Ivanochko, T. S., Ganeshram, R. S., Brummer, G.-J. A., Ganssen, G., Jung, S. J. A., Moreton, S. G., and Kroon, D.: Variations in tropical convection as an amplifier of global climate change at the millennial scale, Earth Planet. Sci. Lett., 235, 302-314, 2005.

Saraswat, R., Lea, D. W., Nigam, R., Mackensen, A., and Naik, D. K.: Deglaciation in the tropical Indian Ocean driven by interplay between the regional monsoon and global teleconnections, Earth Planet. Sci. Lett., 375, 166-175, 2013.

Schulte, S. and Muller, P. J.: Variations of sea surface temperature and primary productivity during Heinrich and Dansgaard-Oeschger events in the northeastern Arabian Sea, Geo-Mar. Lett., 21, 168-175, 2001.

Suthhof, A., Ittekkot, V., and Gaye-Haake, B.: Millennial-scale oscillation of denitrification intensity in the Arabian Sea during the late Quaternary and its potential influence on atmospheric N_2O and global climate, Global Biogeochemical Cycles, 15, 637-650, 2001.

Tierney, J. E., Pausata, F. S. R., and deMenocal, P.: Deglacial Indian monsoon failure and North Atlantic stadials linked by Indian Ocean surface cooling, Nat. Geosci., 9, 46-+, 2016.